Clays and Clay Minerals, Vol. 41, No. 2, 209–218, 1993.

CHANGES IN PARTICLE MORPHOLOGY DURING ILLITIZATION: AN EXPERIMENTAL STUDY

GENE WHITNEY[1] AND BRUCE VELDE[2]

[1]U.S. Geological Survey, MS 904 Box 25046, Denver, Colorado 80225

[2]École Normale Supérieure, 24 rue Lhomond, 75231 Paris, France

Abstract—Smectite was reacted at several temperatures between 200°C and 500°C to produce interstratified illite/smectite (I/S) with different proportions of expandable layers. Dispersed and sedimented products were examined using a transmission electron microscope. Particle size and aspect ratio showed no systematic change as a function of reaction extent during R0 illitization. However, particles exhibited rounded edges during the early stages of the reaction, suggesting some dissolution of primary smectite. Additionally, increasing particle contrast in the electron beam suggests thickening of particles with increasing reaction extent. The thickening of particles is thought to be produced by the nucleation and precipitation of secondary illite layers on primary smectite layers. In the most extensively reacted I/S, particles have become aggregated into clumps or quasicrystals by lateral growth of illite layers. Internal uniformity of crystallographic alignment of individual growing crystals within each aggregate was reflected in the increasing frequency of 60° and 120° interfacial angles within each aggregate. In highly illitic I/S, these aggregates took on an overall euhedral form and became crystallographically contiguous, producing single crystal electron diffraction patterns.

Key Words—Illitization, Morphology, Particle, TEM.

INTRODUCTION

The reaction of smectite to illite via an intermediate interstratified illite/smectite (I/S), commonly called illitization, may be a series of two or more reactions with different reaction rates and reaction mechanisms (Inoue *et al.*, 1988; Whitney and Northrop, 1988; Pollastro, 1985). The first stage of the reaction may produce randomly interstratified I/S, and the second stage may produce ordered (R1 or R3) I/S. There is a general correlation between the extent of the reaction and temperature in natural diagenetic environments. According to the classical view of the reaction, the onset of R0 illitization generally occurs near 50°C, and the R1 stage of illitization begins at about 100°C in Tertiary or older rocks and at somewhat higher temperatures in younger rocks (Pollastro, 1990). According to this view, the early (R0) stage of the illitization reaction is generally associated with early compaction and dewatering of shale, rising organic acid concentrations in pore fluids (Corothers and Kharaka, 1978; Surdam *et al.*, 1989), and the early stages of petroleum generation and migration (Tissot and Welte, 1978). Recent data suggest that the reaction from smectitic I/S to illitic I/S may proceed over a much narrower burial interval than previously thought (Morton, 1985; Freed and Peacor, 1992; Ohr *et al.*, 1991), but details of the reaction remain unclear. The contribution of the illitization reaction and its byproducts to fluid and ion fluxes out of shales, and the consequent effects on fluid pressure or cementation in adjacent rocks cannot be quantitatively assessed without a thorough understanding of the overall reaction. Furthermore, the illitization reaction is thermally driven and is, therefore, potentially useful as a paleotemperature indicator. Thus, it is important to understand as precisely as possible how illitization proceeds. The purpose of the present paper is to investigate mechanisms of illitization by examining morphological changes in I/S particles during experimental smectite-to-illite reactions.

EXPERIMENTAL AND ANALYTICAL METHODS

Changes in clay particle morphology during illitization were studied experimentally using standard hydrothermal techniques (Whitney and Northrop, 1988). Experiments were conducted using K-saturated montmorillonite (Source Clay Mineral Repository sample SWY-1) as starting material. Thirty milligrams of the <0.1 μm fraction (equivalent spherical diameter) was combined with 30 μl of 1.0 N NaCl in a gold capsule and sealed. All samples were weighed before and after hydrothermal treatment to detect leakage; any leaked samples were discarded. Samples were treated at temperatures of 200°C, 250°C, 300°C, 350°C, 450°C, or 500°C for 7 days. A pressure of 100 MPa (1 kbar) was used for all experiments.

After hydrothermal treatment, each sample was gently disaggregated in distilled water in a mortar and pestle. The resulting suspension was placed on a glass slide to produce an oriented specimen for X-ray powder diffraction (XRD) analysis. Each sample was analyzed by XRD after being air-dried and after saturation with ethylene glycol (overnight at 60°C in glycol vapor). The proportion of smectite and illite layers in

Copyright © 1993, The Clay Minerals Society

https://doi.org/10.1346/CCMN.1993.0410209 Published online by Cambridge University Press

I/S products was determined using the algorithm of Reynolds (1980).

Materials were prepared for transmission electron microscope (TEM) analysis by suspending 5.0 mg of each sample in 9.0 ml of distilled water and dispersing with a probe-type ultrasonic disaggregator for 1 min. Samples were further diluted by placing 20 μl of the resulting suspension in 10 ml of distilled water. One drop of this second suspension was placed on a carbon-coated copper grid and allowed to dry at 25°C for presentation in a Philips 390 TEM* or a JEOL 1200EX TEM operating at 80 kV to 120 kV. Great care was taken to ensure that all samples experienced the same dispersal and mounting treatments.

TEM photomicrographs were digitized using a flatbed scanner, and quantitative analysis of particle size and shape was performed using image analysis software (Image, v. 1.37, public domain software authored by Wayne Rasband, National Institute of Health) on a Macintosh II computer. The particle outlines were traced by hand on the computer screen with a mouse-driven drawing tool, and maximum length, width, and circumference were calculated by the image analysis software. Outlines of between 200 and 300 particles per sample were measured. The particle areas and aspect ratios were calculated and compared using histograms.

RESULTS

Mineralogy and expandability trends

Expandability and calculated fundamental particle thickness measurements are tabulated in Table 1 along with other experimental parameters. Increasing reaction extent with increasing temperature is demonstrated by the decrease in percent expandable layers in the I/S (Figure 1). Each sample represents a new run at a different temperature, so the more extensively reacted high-temperature experiments do not necessarily represent simple extensions of the low-temperature reactions. Small amounts of quartz or cristobalite were produced in the higher-temperature experiments.

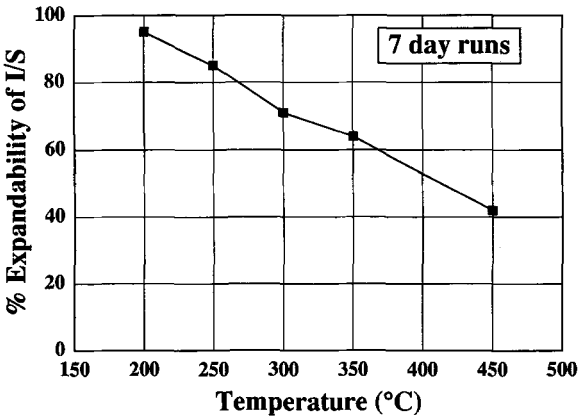


Figure 1. Plot of the expandability of interstratified I/S versus the experimental run temperature for 7-day runs. When the starting smectite is included, the range of expandability extends from 100% to 10%.

Particle characteristics and morphology

The characteristics of individual clay particles and relationships among adjacent particles were documented for samples exhibiting a range of expandability or reaction extent. Trends in particle dimensions during the R0 stage of illitization are summarized in histograms in Figure 2. The dominant feature of these plots is that there is almost no systematic change in particle dimensions (length or width) during the R0 stage of illitization. No histograms are presented for R1 or R3 illitization because clumping or coalescence of small particles made it very difficult to measure dimensions of individual particles. Within a coalescing crystallite, individual particle boundaries became difficult to discern. Although a few lath-shaped particles formed near 50% expandability in our experiments, there was no significant change in morphology to lath-shaped or fibrous particles like those seen in some natural materials (Inoue *et al.*, 1987, 1988; Pollastro, 1985).

Although there was little change in particle dimensions during R0 illitization, subtle changes occurred in the shapes of individual particles. The morphology of

* Brand names used here and elsewhere are for descriptive purposes only and do not constitute endorsement by the U.S. Geological Survey.

Table 1. Run conditions and particle measurements for experimentally produced I/S.

Sample	Run time (days)	Temp. (°C)	% Exp.	Calculated particle thickness (nm)	Mean area (μm²)	Mean length (μm)	Mean width (μm)	Aspect ratio	% Covered
SWY1	0	—	100	1.00	0.036	0.247	0.139	1.95	71
PN12	7	200	95	1.05	0.036	0.260	0.152	1.92	64
PN8	7	300	71	1.40	0.033	0.239	0.140	1.88	49
PN9	7	350	64	1.56	0.035	0.243	0.140	1.93	46
PN10	7	450	42	2.38	0.038	0.256	0.150	1.87	43
PN14	10	400	42	2.38	0.030	0.243	0.128	2.27	42

https://doi.org/10.1346/CCMN.1993.0410209 Published online by Cambridge University Press

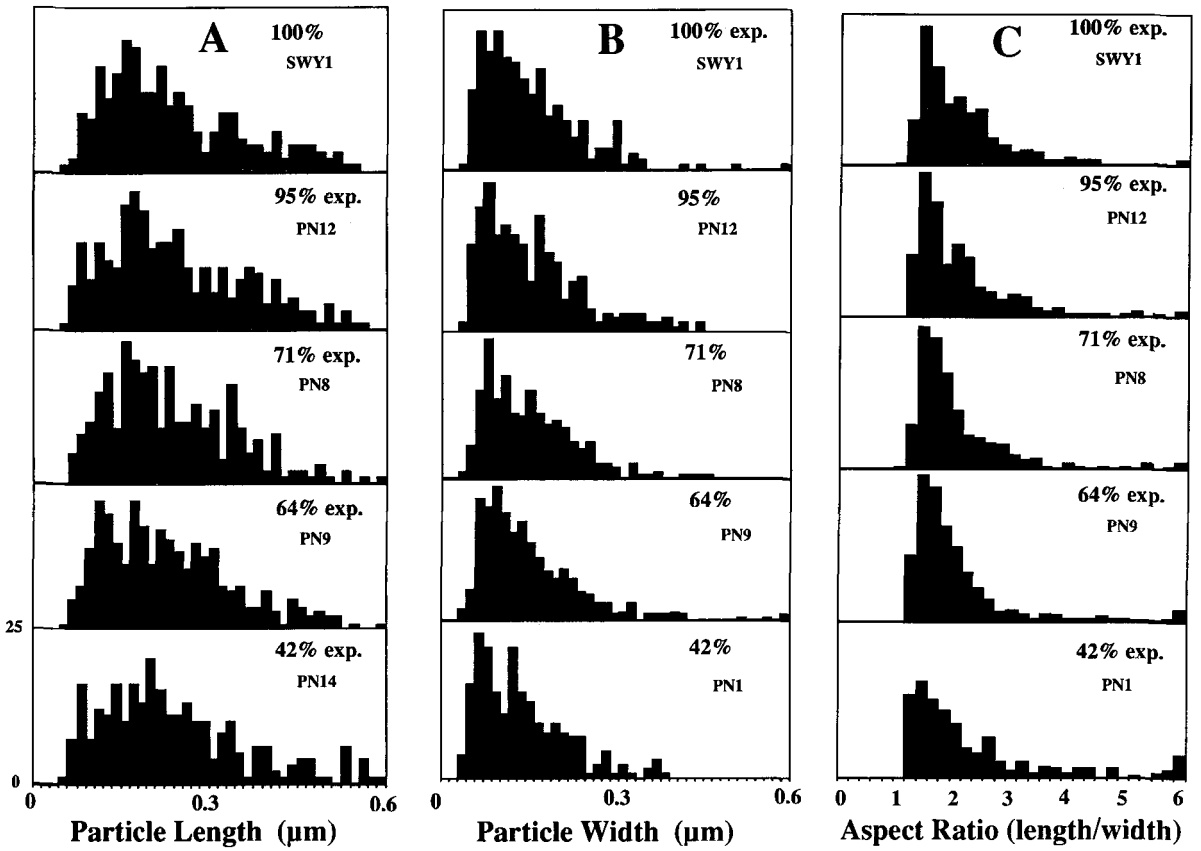


Figure 2. Histogram plots of A) particle length, B) particle width, and C) aspect ratio *vs* reaction progress. There is no significant change in dimensions of individual particles during the illitization reaction.

particles changed from the irregular and ragged outline of original smectite flakes to rounded or euhedral forms in the I/S run products (Figure 3).

In addition to subtle changes in particle shape, individual particles grew thicker and formed aggregates in the more extensively reacted samples (Figure 4). These particle aggregates are quite cohesive and resist disruption by ultrasonic probe. The degree to which aggregation occurred can be measured by the proportion of substrate covered by particles (precisely the same mass of material was suspended for each sample). Because of extremely low contrast exhibited by the thin smectite particles, image analysis software was used to generate binary images (black where particles exist, white where none exist) of several TEM photomicrographs of each sample to measure the areas covered by clay particles (Figure 5). The binary images clearly show the reduction in area covered by particles as the reaction proceeded, measured as a percent of total area within the TEM photomicrograph field of view. The binary images demonstrate that the percentage of the substrate covered by clay particles decreased as the percent illite in I/S increased (Table 1).

An additional significant morphological change is the increased development of 60° and 120° angles along particle edges in the clay aggregates as the reaction proceeded (Figure 6). Angular relationships among particle edges and boundaries are random in the starting smectite particles, but the interfacial angles on individual particles and within aggregates of particles become increasingly regular, reflecting the 60° and 120° crystal boundaries on trigonal or hexagonal (or pseudohexagonal or pseudotrigonal) crystals. In more advanced stages of illitization, the strong development of 60° and 120° angles produces a rhombohedral outline in the total aggregate as individual particles coalesce into a single larger quasicrystal (Figure 7). Within such a quasicrystal, both rounded and euhedral component particles are distinguishable.

SAD patterns for unreacted and reacted clays reveal the stacking arrangement of the layers. The streaked spots in the electron diffraction pattern for unreacted smectite (Figure 8A, showing SAD for smectite viewed in Figure 3A) demonstrates that the smectite particles are not completely randomly stacked, but rather have some coherence of layers in packets. For a partially reacted, 42% expandable I/S (Figure 8B, showing SAD for I/S viewed in Figure 4C), the SAD pattern is that

https://doi.org/10.1346/CCMN.1993.0410209 Published online by Cambridge University Press

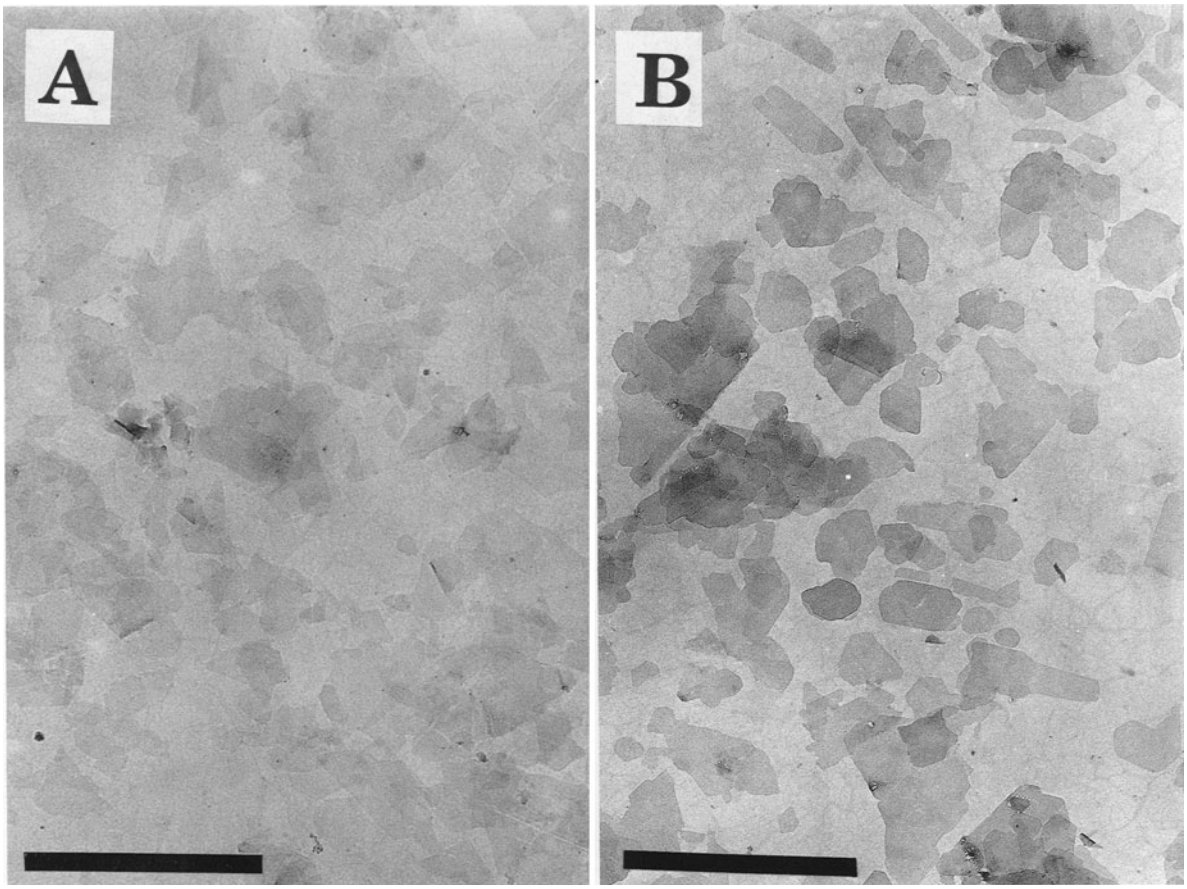


Figure 3. TEM photos showing changes in the degree of rounding during the illitization reaction. The starting smectite (A) has very angular particles, whereas the partly reacted (71% expandable) I/S (B) has more rounded particles, suggesting some dissolution at the edges. Scale bar is 1 μm.

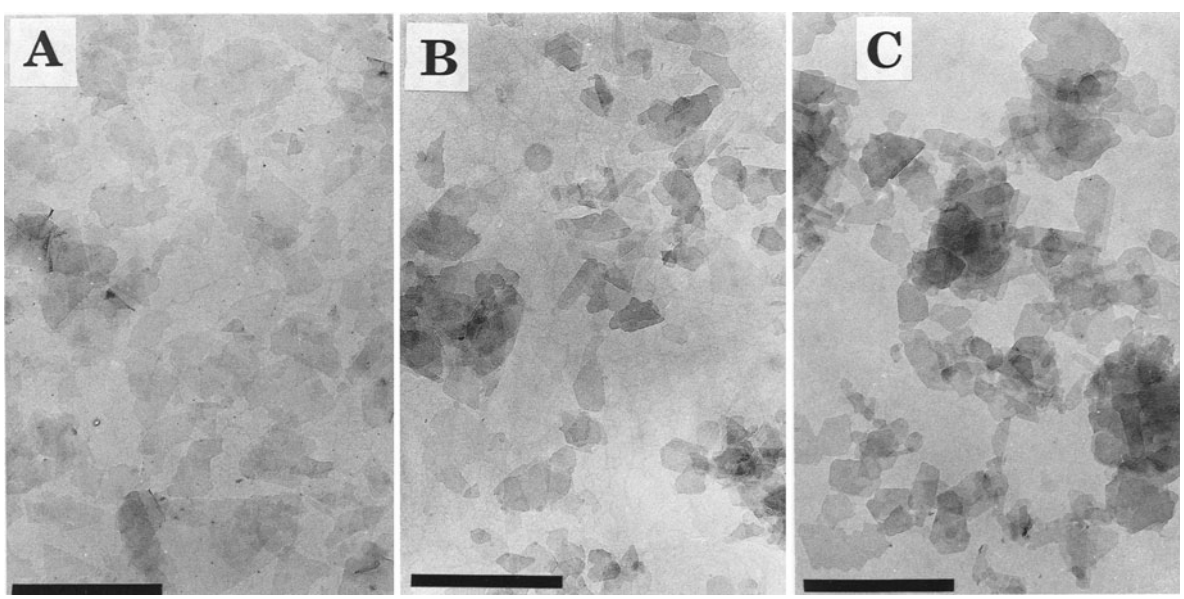


Figure 4. TEM micrographs of I/S run products showing the adhering of individual particles into aggregates. These aggregates were not disrupted by the ultrasonic treatment. A) 100% expandable smectite starting material, B) 71% expandable I/S, C) 42% expandable I/S. Scale bar is 1 μm.

https://doi.org/10.1346/CCMN.1993.0410209 Published online by Cambridge University Press

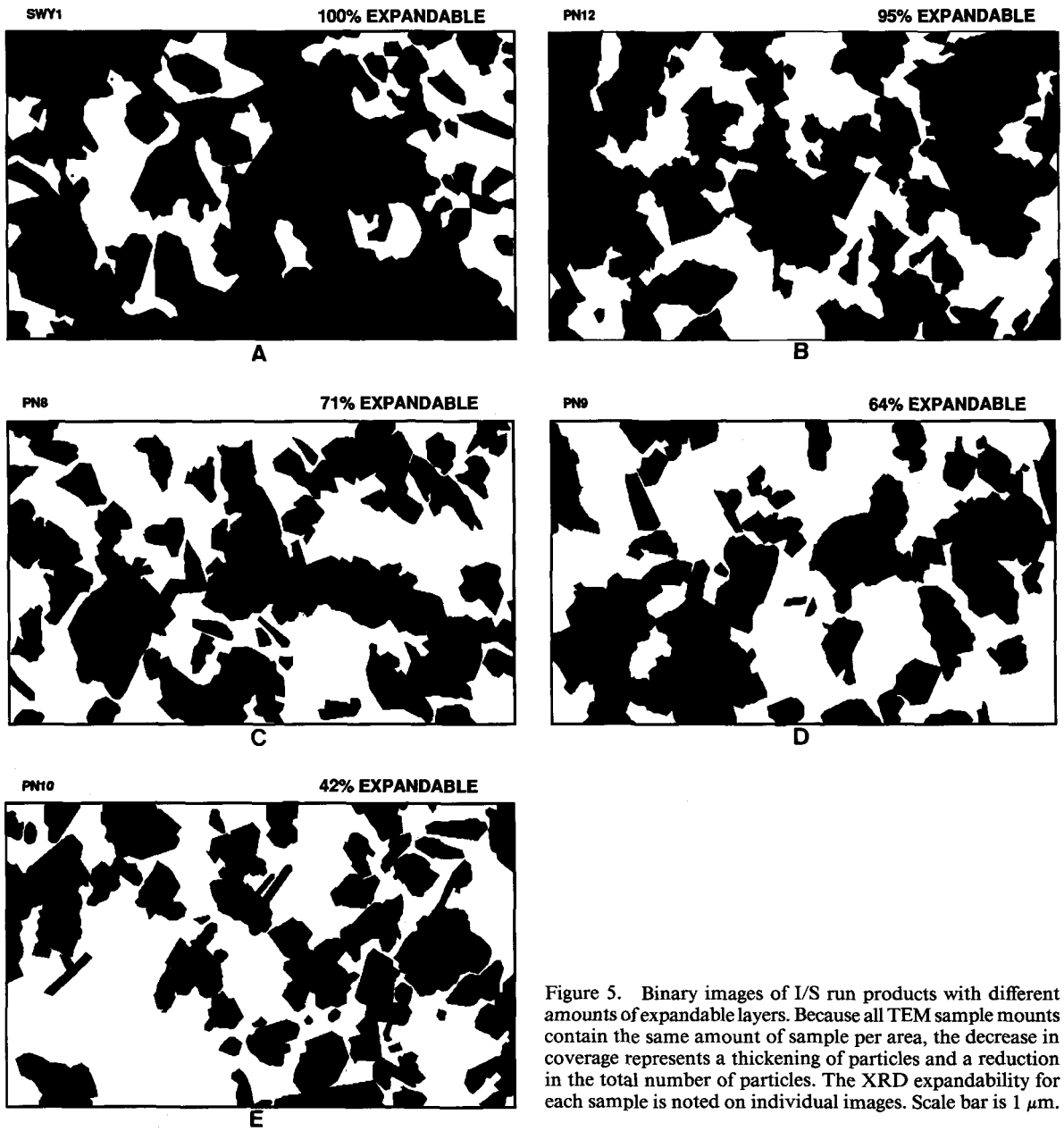


Figure 5. Binary images of I/S run products with different amounts of expandable layers. Because all TEM sample mounts contain the same amount of sample per area, the decrease in coverage represents a thickening of particles and a reduction in the total number of particles. The XRD expandability for each sample is noted on individual images. Scale bar is 1 μm.

of a single crystal, demonstrating well-defined coherence of layers within a particle.

INTERPRETATION AND DISCUSSION

Both dissolution-precipitation mechanisms and solid-state transformation mechanisms have been suggested to explain the reaction of smectite to illite via interstratified intermediate I/S clay minerals (e.g., Nadeau *et al.*, 1984a, 1984b, 1986; Ahn and Peacor, 1986; Whitney and Northrop, 1988; Inoue *et al.*, 1988; Pollastro, 1985). The morphological data presented here suggest that illitization involves dissolution of primary smectite particles and precipitation of illitic material (not necessarily discrete illite crystals) even in the early stages of the reaction. Based on the morphology and physical association of particles in these experiments, we propose that the illitization reaction may progress in four steps:

1) Dissolution of primary smectite.

2) Epitaxial nucleation and growth of illite layers on smectite substrate.

3) Coalescence of thin illite particles to form aggregates (quasicrystals).

4) Infilling and syntaxial growth of quasicrystals to form homogeneous crystals of illite.

Each of these steps is discussed in detail below.

https://doi.org/10.1346/CCMN.1993.0410209 Published online by Cambridge University Press

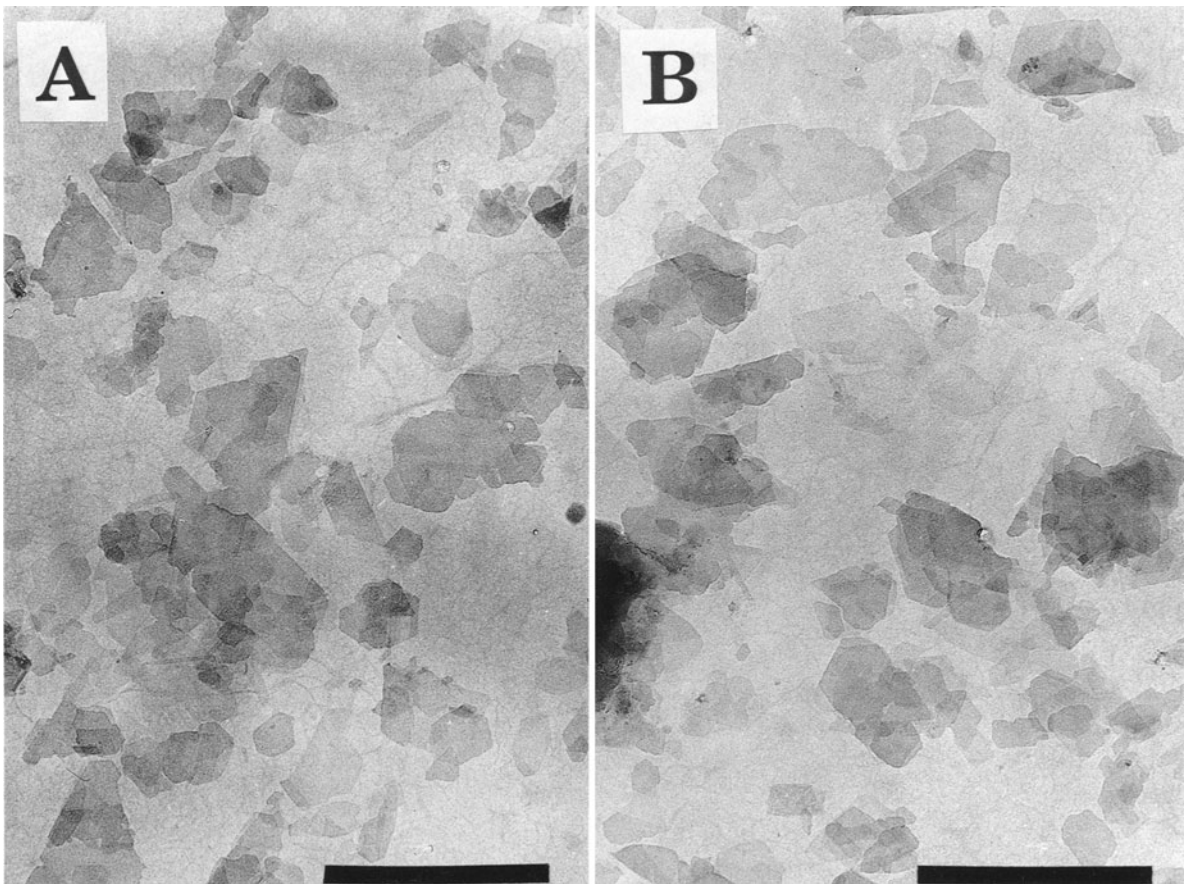


Figure 6. TEM micrographs of I/S showing the appearance of linear edges bounded by 60° and 120° angles at particle boundaries and within aggregates. The regularity of these angles results from crystal growth processes within aggregates. Both A) and B) are 71% expandable I/S. Scale bar is 1 μm.

Dissolution of primary smectite

Dissolution of the primary smectite is reflected in the rounding of particles and in the decrease in the total area of substrate covered as the reaction proceeded. The number of particles decreased as the thickness of particles increased. Because the experiments were conducted in closed systems, particles could grow only by dissolution of other particles. Dissolution of aluminous smectite is expected because it is unstable at the temperatures of these experiments (Eberl *et al.*, 1978), and the dissolution is rapid because of the very small grain size (<0.1 μm equivalent spherical diameter), the very small thickness of each smectite layer (≈10 Å), and the resulting high surface area of the starting smectite.

Dissolution of particles causes a decrease in particle size whereas crystal growth causes particle size to increase. For a population of clay particles in a closed system (including these experiments), mass balance constraints require that, if some of these platy particles become thicker, others must decrease in size (thickness or lateral dimensions) and/or be reduced in number. We have observed that the number of particles decreased while they increased in thickness. Some of the mass required for thickening particles clearly comes from the particles that have dissolved. But how is that mass transferred without changing the size distribution of the population of particles? It is difficult to imagine a clay flake dissolving without reducing its lateral dimensions in the process. If our hypothesis is correct, there must exist a balance between the reduction in dimensions of primary particles (including total dissolution of some), nucleation of new small particles, and the increase in the dimensions of small particles to account for the overall lack of change in the distribution of sizes. Because rounding of particles and coalescence of particles proceed at the same time as the dissolution and thickening processes, it remains difficult to define mass transfer during R0 illitization.

Epitaxial nucleation and growth of illite on smectite substrate

The thickening of particles observed in our experiments may result from growth of new illite layers on

https://doi.org/10.1346/CCMN.1993.0410209 Published online by Cambridge University Press

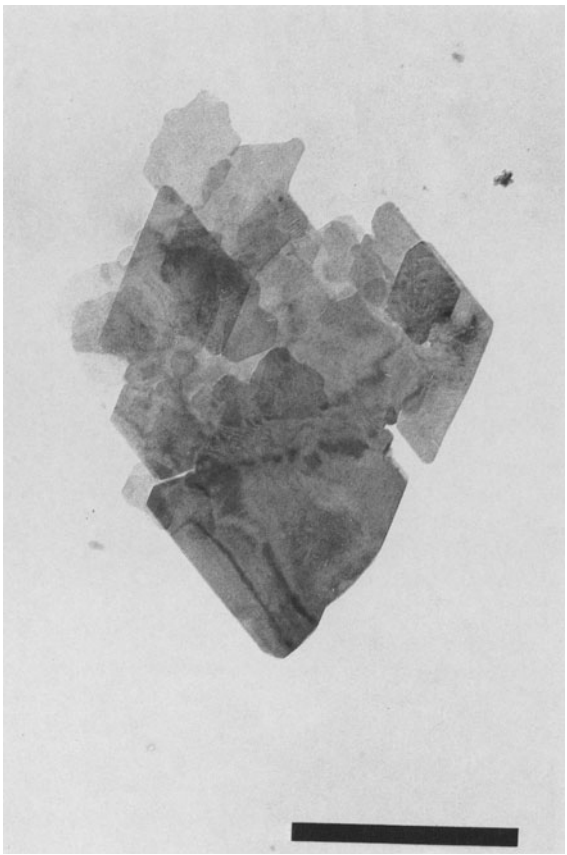


Figure 7. A coalescent particle of 10% expandable I/S showing both rounded (dissolving) and euhedral (crystallizing) particles within the aggregate. The overall shape of the aggregate approaches a rhombic outline of a large illite particle though it is composed of a mosaic of small particles.

old smectite layers. The dissolution of smectite, combined with the relatively small fluid-to-solid ratio (1:1), may quickly generate a fluid that is supersaturated relative to stable secondary minerals such as illite. This experimental system contained little free pore water (Whitney, 1990), so nucleation of new illite layers would be constrained to the surface or interlayer space of smectite particles.* The surface of Al-smectite is probably a favorable nucleation site for illite because the 2:1 silicate layers of the two minerals have similar compositions and virtually identical a-b crystallographic dimensions, and nucleation is facilitated when the surface energies of the existing substrate and the newly precipitated phase are similar (Wollast, 1971). Thus, the smectite layer could serve as an energetically favorable nucleation site, or template, for two dimensional nucleation of illite layers. Sunagawa *et al.* (1975) have suggested such two-dimensional nucleation as a growth mechanism in phyllosilicates in highly supersaturated metamorphic systems.

An alternative to direct precipitation of illite is growth of illite around a smectite nucleus. Small smectite particles in surface-to-surface contact with larger smectite particles may have served as nuclei for the overgrowth of illite layers (Figure 9) in a manner similar to the crystallization of calcite on aragonite nuclei (Wollast, 1971). Such a mechanism has been suggested for the illitization reaction in natural systems (Pollastro, 1985). Nucleation may be facilitated by syntaxial growth around the smectite nucleus, and lateral growth of the illite layer could be accelerated by the epitaxial contact with the smectite substrate. Gaultier and Mamy (1979), Banfield *et al.* (1991), and Freed and Peacor (1992) have shown that smectite layers are frequently not completely randomly oriented (turbostratic) with respect to adjacent layers but, rather, that adjacent layers tend to align themselves so that the hexagonal cavities in the base of the silicate layers are superimposed. Our SAD data clearly demonstrates that at least some of the smectite layers in our experiments are coherently stacked within packets, providing a favorable setting for such nucleation to occur. If adjacent silicate layers are keyed on interlayer potassium ions, the surface area (and therefore the surface free energy) of the two-layer structure is reduced relative to the same two particles existing separately, and the two-layer pair is stabilized (Eberl *et al.*, 1986; Plançon *et al.*, 1979). Conversely, small, non-aligned layers would be less stable and would therefore dissolve more readily.

In natural environments, such alignment between smectite layers can be accentuated by wetting and drying (Andreoli *et al.*, 1989; Eberl *et al.*, 1986; Plançon *et al.*, 1979) or changes in fluid chemistry (Quirk and Aylmore, 1971; Whalley and Mullins, 1991). Thus, chemical and physical conditions within the depositional environment of smectitic sediment may affect the subsequent illitization reaction. In one possible example of this effect, Howard (1987, 1991) showed that laminated shales from Texas Gulf Coast sediments were measurably more illitic than chemically identical massive shales from the same section. Our interpretation of this data is that the increased frequency of face-to-face contact between primary smectite layers in the laminated shales facilitated nucleation and growth of illite layers and thereby accelerated the illitization reaction.

Coalescence of thin illite particles to form aggregates (quasicrystals)

In the more extensively reacted samples, particles assumed a hexagonal or rhombohedral morphology and impinged upon adjacent growing layers. Because these experiments represent different runs at different

* Because smectite may swell between all 2:1 silicate layers, the difference between particle surfaces and interlayer space of smectites is small in a compressed smectite-water mixture.

https://doi.org/10.1346/CCMN.1993.0410209 Published online by Cambridge University Press

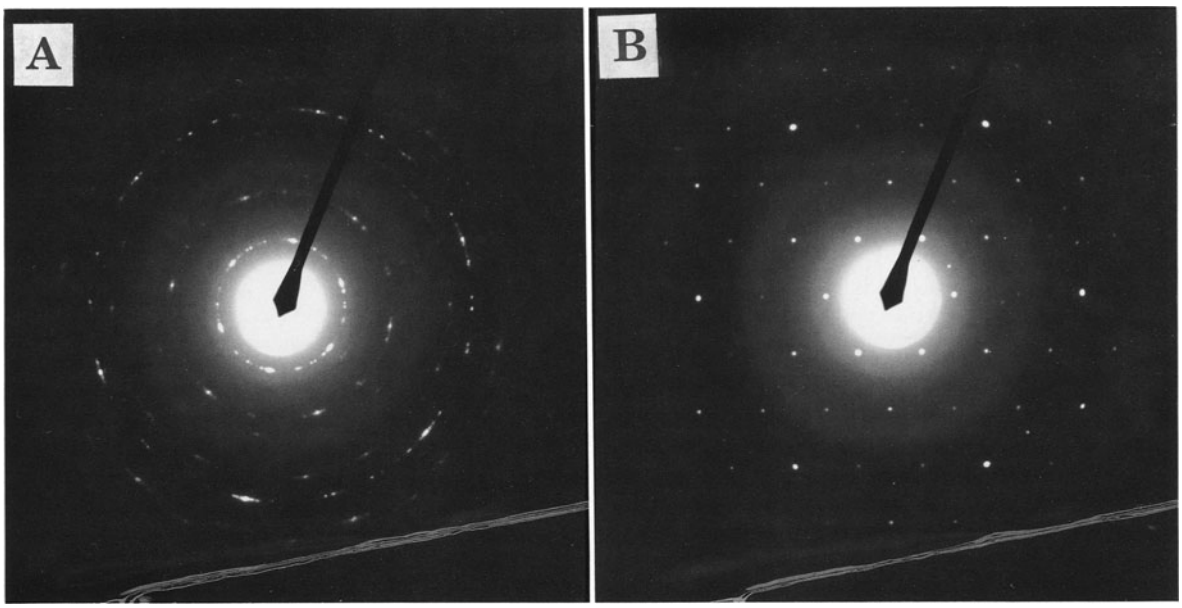


Figure 8. Selected area electron diffraction patterns for A) unreacted smectite (material pictured in Figure 3A) and B) 42% expandable I/S (material pictured in Figure 4C). The streaked spots in the smectite pattern demonstrate that the layers are not completely randomly arranged, but have some coherence of layers in packets. The well-defined spots for the I/S show that a particle of the 42% expandable I/S produces a single crystal diffraction pattern.

temperatures, rather than a continuous series at a single temperature, it is not possible to unequivocally identify evolution from one morphology to another. However, if aligned particles continued to grow and non-aligned smectite particles dissolved, the syntaxial lateral growth of illite layers within an aggregate would tend to be along similar crystallographic axes. Thus, the development of the 60° and 120° angles in the particle aggregates strongly suggests crystal growth and possibly crystal coalescence. The SAD data for such samples (Figure 8B) show well-defined single crystal patterns of illite. Relict smectite layers that had been stabilized by the early-formed epitaxial illite layers may have dissolved and been replaced by new illite layers. The proportion of adjacent illite layers in the stack would thereby increase, and the I/S would become progressively more illitic. As the crystals grew laterally, individual particles would become increasingly intergrown and the aggregates would become inseparable units as shown in the cartoon in Figure 10. Figure 7 shows an example of such a coalescing aggregate particle.

Infilling and syntaxial growth of aggregates

The final stage of the dissolution and recrystallization process is the reduction of surface area by preferential dissolution of individual particles or small aggregates followed by growth of larger and more compact aggregates (quasicrystals) with a smaller surface to volume ratio. These coalescent aggregates grow together to form crystallographically contiguous and morphologically simpler crystals.

Ostwald ripening has been suggested as the process

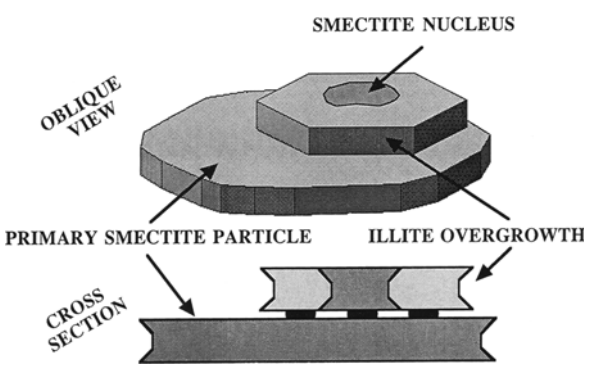


Figure 9. Cartoon representation of a secondary illite layer nucleating on a primary smectite layer. In some cases, small smectite layers may serve as nuclei for illite layer overgrowths.

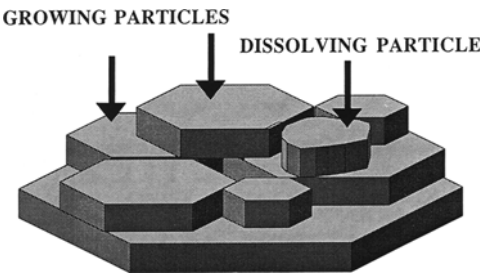


Figure 10. Sketch of I/S aggregate made up of smectite layers, illite layers, and two-layer hybrid particles. Euhedral particles represent growing illite layers, rounded particles represent dissolving smectite or illite.

https://doi.org/10.1346/CCMN.1993.0410209 Published online by Cambridge University Press

by which small illite crystals dissolve and feed the growth of larger crystals, thereby reducing surface free energy of the system while maintaining a single mineral composition (Baronnet, 1984; Eberl *et al.*, 1990; Eberl and Środoń, 1988; Morse and Casey, 1988). Because Ostwald ripening refers to a monominerallic system, the illitization reaction cannot be viewed as Ostwald ripening until all crystals have the same uniform illite composition. Because primary smectite layers probably persist even when the I/S is highly illitic, Ostwald ripening is probably not the dominant process during illitization until virtually all of the relict smectite layers have dissolved.

Our experiments show that many illite "crystals" are not independent euhedral crystals, but occur in polycrystalline aggregates. These aggregates may exhibit expandable layers within the aggregate particle, as suggested by Środoń *et al.* (1990). Thus, the formation of more illitic I/S requires more than simple dissolution of isolated fine illite particles. In order to minimize surface free energy within populations of mosaic aggregates, those aggregates with higher total surface area dissolve preferentially and nourish the growth and infilling of more compact aggregates or single crystals. The dynamics of this variant of the "ripening" process are undoubtedly much more complex than simple dissolution of small particles, and the modeling of the reaction becomes extremely difficult. Furthermore, the set of nucleation and crystal growth processes described here is much more relevant in shales than sandstones because our experimental reactions proceeded in a compressed mass of clay, whereas illite growing in fluid-dominated, open pore spaces may proceed by a different set of nucleation and crystal growth processes.

SUMMARY AND CONCLUSIONS

Morphological changes in I/S during the illitization reaction suggest that dissolution and precipitation are important processes during the earliest stages of the reaction. Based on our TEM data, we interpret the reaction to proceed in four steps: 1) dissolution of primary smectite, 2) epitaxial nucleation of illite on smectite substrate, 3) coalescence of thin illite particles to form aggregates, and 4) infilling and syntaxial growth of aggregates to form homogeneous crystals of illite. The overall effect is growth of large illite particles from small smectite particles, but these experimental data add to a growing body of information suggesting that the processes by which illitization proceeds are more complex than formerly believed.

ACKNOWLEDGMENTS

We thank Mme. André of the University of Paris for training, for the use of the TEM, and for photographic developing of the negatives and prints. Prof. Alain Baronnet, of the Center for Crystal Growth Studies at Marseille, helped with examination of run products using selected-area electron diffraction. We thank Elf Technologies Inc. for funding this research and École Normale Supérieure, Paris, for logistical support. G. W. is grateful to the USGS Evolution of Sedimentary Basins Program for supporting portions of this research. We thank James Howard and an anonymous reviewer for materially improving the manuscript.

REFERENCES

Ahn, J. H. and Peacor, D. R. (1986) Transmission and analytical electron microscopy of the smectite-to-illite transition: *Clays & Clay Minerals* **34,** 165–179.

Andreoli, C. Y., Robert, M., and Pons, C. H. (1989) First steps of smectite-illite transformation with humectation and desiccation cycles: *Applied Clay Science* **4,** 423–435.

Banfield, J. F., Jones, B. F., and Veblen, D. R. (1991) An AEM-TEM study of weathering and diagenesis, Abert Lake, Oregon: II. Diagenetic modification of the sedimentary assemblage: *Geochim. et Cosmochim. Acta* **55,** 2795–2810.

Baronnet, A. (1984) Growth kinetics of the silicates: A review of basic concepts: *Fortsch. Miner.* **62,** 187–232.

Corothers, W. W. and Kharaka, Y. K. (1978) Aliphatic acid anions in oil-field waters—Implications for origin of natural gas: *Am. Assoc. Petroleum Geol. Bull.* **62,** 2441–2453.

Eberl, D. D. and Środoń, J. (1988) Ostwald ripening and interparticle-diffraction effects for illite crystals: *Amer. Mineral.* **73,** 1335–1345.

Eberl, D. D., Środoń, J., Kralik, M., Taylor, B. E., and Peterman, Z. (1990) Ostwald ripening of clays and metamorphic rocks: *Science* **248,** 474–477.

Eberl, D. D., Środoń, J., and Northrop, H. R. (1986) Potassium fixation in smectite by wetting and drying: in *Geochemical Processes at Mineral Surfaces,* J. A. Davis and K. F. Hayes, eds., American Chemical Society, Washington, D.C., 296–326.

Eberl, D. D., Whitney, G., and Khoury, H. (1978) Hydrothermal reactivity of smectite: *Amer. Mineral.* **63,** 401–409.

Freed, R. L. and Peacor, D. R. (1992) Diagenesis and the formation of authigenic illite-rich I/S crystals in Gulf Coast shales: TEM study of clay separates: *Jour. Sed. Petr.* **62,** 220–234.

Gaultier, J. P. and Mamy, J. (1979) Evolution of exchange properties and crystallographic characteristics of biionic K-Ca montmorillonite submitted to alternate wetting and drying: in *Proc. Int. Clay Conf. 1978, Oxford,* M. M. Mortland and V. C. Farmer, eds., Developments in Sedimentology 27, Elsevier Scientific Publishing Company, Amsterdam, 167–175.

Howard, J. J. (1987) Influence of shale fabric on illite/smectite diagenesis in the Oligocene Frio Formation, South Texas: in *Proc. Inter. Clay Conf. 1985, Denver,* L. G. Schultz, H. van Olphen, and F. A. Mumpton, eds., The Clay Minerals Society, Bloomington, Indiana, 144–150.

Howard, J. J. (1991) Porosimetry measurement of shale fabric and its relationship to illite-smectite diagenesis: *Clays & Clay Minerals* **39,** 355–361.

Inoue, A., Kohyama, N., Kitagawa, R., and Watanabe, T. (1987) Chemical and morphological evidence for the conversion of smectite to illite: *Clays & Clay Minerals* **35,** 111–120.

Inoue, A., Velde, B., Meunier, A., and Touchard, G. (1988) Mechanism of illite formation during smectite-to-illite conversion in a hydrothermal system: *Amer. Mineral.* **73,** 1325–1334.

Morse, J. W. and Casey, W. H. (1988) Ostwald processes and mineral paragenesis in sediments. *Amer. Jour. Sci.* **288,** 537–560.

https://doi.org/10.1346/CCMN.1993.0410209 Published online by Cambridge University Press

Morton, J. P. (1985) Rb-Sr evidence for punctuated illite/smectite diagenesis in the Oligocene Frio Formation, Texas Gulf Coast: *Geol. Soc. Amer. Bull.* **96,** 114–122.

Nadeau, P. H. and Bain, D. C. (1986) Composition of some smectites and diagenetic illitic clays and implications for their origin: *Clays & Clay Minerals* **34,** 455–464.

Nadeau, P. H., Wilson, M. J., McHardy, W. J., and Tait, J. M. (1984a) Interstratified clays as fundamental particles: *Science* **225,** 923–925.

Nadeau, P. H., Wilson, M. J., McHardy, W. J., and Tait, J. M. (1984b) Interparticle diffraction: A new concept for interstratified clays: *Clay Miner.* **19,** 757–769.

Ohr, M., Halliday, A. N., and Peacor, D. R. (1991) Sr and Nd isotopic evidence for punctuated clay diagenesis, Texas Gulf Coast: *Earth Planet. Sci. Lett.* **105,** 110–126.

Plançon, A., Besson, G., Gaultier, J. P., Mamy, J., and Tchoubar, C. (1979) Qualitative and quantitative study of a structural reorganization in montmorillonite after potassium fixation: in *Int. Clay Conf. 1978, Oxford,* M. M. Mortland and V. C. Farmer, eds., Developments in Sedimentology 27, Elsevier Scientific Publishing Company, Amsterdam, 45–54.

Pollastro, R. M. (1985) Mineralogical and morphological evidence for the formation of illite at the expense of illite/smectite: *Clays & Clay Minerals* **33,** 265–274.

Pollastro, R. M. (1990) The illite/smectite geothermometer—Concepts, methodology, and application to basin history and hydrocarbon generation: in *Applications of Thermal Maturity Studies to Energy Exploration,* V. F. Nuccio and C. E. Barker, eds., Society of Economic Paleontologists and Mineralogists, Tulsa, 1–18.

Quirk, J. P. and Aylmore, L. A. G. (1971) Domains and quasi-crystalline regions in clay systems: *Soil Sci. Soc. Amer. Proc.* **35,** 652–654.

Reynolds Jr., R. C. (1980) Interstratified clay minerals: in *Crystal Structures of Clay Minerals and Their X-ray Identification,* G. W. Brindley and G. Brown, eds., Mineralogical Society, London, 249–304.

Środoń, J., Andreoli, C., Elsass, F., and Robert, M. (1990) Direct high-resolution transmission electron microscopic measurement of expandability of mixed-layer illite/smectite in bentonite rocks: *Clays & Clay Minerals* **38,** 373–379.

Sunagawa, I., Koshino, Y., Asakura, M., and Yamamoto, T. (1975) Growth mechanisms of some clay minerals: *Fortschr. Miner.* **52,** 217–224.

Surdam, R. C., Crossey, L. J., Hagen, E. S., and Heasler, H. P. (1989) Organic-inorganic interactions and sandstone diagenesis: *Am. Assoc. Petroleum Geol. Bull.* **73,** 1–23.

Tissot, B. P. and Welte, D. H. (1978) *Petroleum Formation and Occurrence,* Springer-Verlag, New York, 538 pp.

Whalley, W. R. and Mullins, C. E. (1991) Effect of saturating cation on tactoid size distribution in bentonite suspensions: *Clay Miner.* **26,** 11–17.

Whitney, G. (1990) Role of water in the smectite-to-illite reaction: *Clays & Clay Minerals* **38,** 343–350.

Whitney, G. and Northrop, H. R. (1988) Experimental investigation of the smectite to illite reaction—Dual reaction mechanisms and oxygen-isotope systematics: *Amer. Mineral.* **73,** 77–90.

Wollast, R. (1971) Kinetic aspects of the nucleation and growth of calcite from aqueous solutions: in *Carbonate Cements,* O. P. Bricker, ed., The Johns Hopkins Press, Baltimore, 264–273.

(Received 18 March 1993; accepted 19 March 1993; Ms. 2351)

https://doi.org/10.1346/CCMN.1993.0410209 Published online by Cambridge University Press